North Atlantic Natural Variability Modulates Emergence of Widespread Greenland Melt in a Warming Climate

L. Hahn[1] (iD), C. C. Ummenhofer[1] (iD), and Y.-O. Kwon[1] (iD)

[1]Physical Oceanography Department, Woods Hole Oceanographic Institution, Woods Hole, MA, USA

Abstract Record-breaking melt over Greenland in recent decades is linked not only to climate change but also to natural variability, including persistent atmospheric high-pressure conditions in the negative phase of the North Atlantic Oscillation and warm North Atlantic Ocean temperatures during the positive phase of the Atlantic Multidecadal Oscillation. However, the relative importance of natural variability for Greenland melt under varying degrees of greenhouse forcing is still unclear. Using reanalysis data and a large ensemble of climate model simulations, we find that a negative North Atlantic Oscillation and positive Atlantic Multidecadal Oscillation consistently promote heightened summer melt under various forcing conditions. Moreover, timing of widespread 21st century Greenland melt varies considerably between ensemble members due to different phasing of these modes of natural variability. These results indicate the importance of natural modes of variability across a range of external forcing conditions for interannual melt variability and the emergence of widespread Greenland melt.

Plain Language Summary Extreme Greenland Ice Sheet melt is partly driven by climate change, as rising greenhouse gas concentrations promote warmer temperatures, especially for the Arctic region. However, natural fluctuations in the climate system can also promote Greenland melt. In particular, persistent high-pressure systems in the atmosphere over the region and warm North Atlantic Ocean temperatures have been linked to enhanced Greenland melt in recent decades. Yet the importance of these natural oscillations for melt in the past and future remains unclear. We use a series of climate model simulations to show that high-pressure conditions and a warm North Atlantic Ocean consistently promote heightened summer melt under various warming scenarios for the past and future. Additionally, the timing of widespread Greenland melt in the 21st century depends on the timing of these modes of natural variability.

1. Introduction

Greenland Ice Sheet (GrIS) meltwater production is expected to contribute significantly to global sea level rise (Fettweis, Franco, et al., 2013; Shepherd et al., 2012) and may weaken the Atlantic meridional overturning circulation by suppressing deep convection (Böning et al., 2016; Oltmanns et al., 2018; Rahmstorf et al., 2015), motivating efforts to understand what drives GrIS melt. Recent work highlights the dominant role of atmospheric and oceanic variability, specifically the North Atlantic Oscillation (NAO) and the related Greenland Blocking Index (GBI; Box et al., 2012; Chylek et al., 2004; Ding et al., 2014; Fettweis, Hanna, et al., 2013; Häkkinen et al., 2014; Hanna et al., 2014, 2013; Lim et al., 2016; McLeod & Mote, 2016; Tedesco et al., 2016), as well as the Atlantic Multidecadal Oscillation (AMO; Chylek et al., 2009; Hanna et al., 2013; McLeod & Mote, 2016; Straneo & Heimbach, 2013), in promoting Greenland surface melt.

In recent decades, the most extreme melt seasons exhibited significant high-pressure blocking anomalies over Greenland associated with positive GBI values and the negative phase of the NAO (Fettweis, Hanna, et al., 2013; Tedesco et al., 2016; Figure 1), with significant increases in summer Greenland blocking since 1981 (Hanna et al., 2016, Hanna, Hall, et al., 2018). These prolonged atmospheric blocking episodes may promote melt via northward advection of warm air over west Greenland (Fettweis et al., 2011), adiabatic warming of sinking air associated with anticyclonic circulation anomalies (Ding et al., 2017), or radiative impacts of cloud cover changes resulting from blocking conditions (Hofer et al., 2017; Lim et al., 2016). The positive AMO phase, defined by anomalously warm North Atlantic sea surface temperatures (SSTs) after the global warming signal has been removed, is also significantly linked to surface melt over the entire GrIS potentially due to a strong connection between the AMO and NAO (Hanna et al., 2013; McLeod & Mote, 2016), although the direction of causality for this connection is debated (Gastineau & Frankignoul, 2015; Häkkinen et al., 2011; Peings & Magnusdottir, 2014). With atmospheric and oceanic variability established as dominant drivers of Greenland
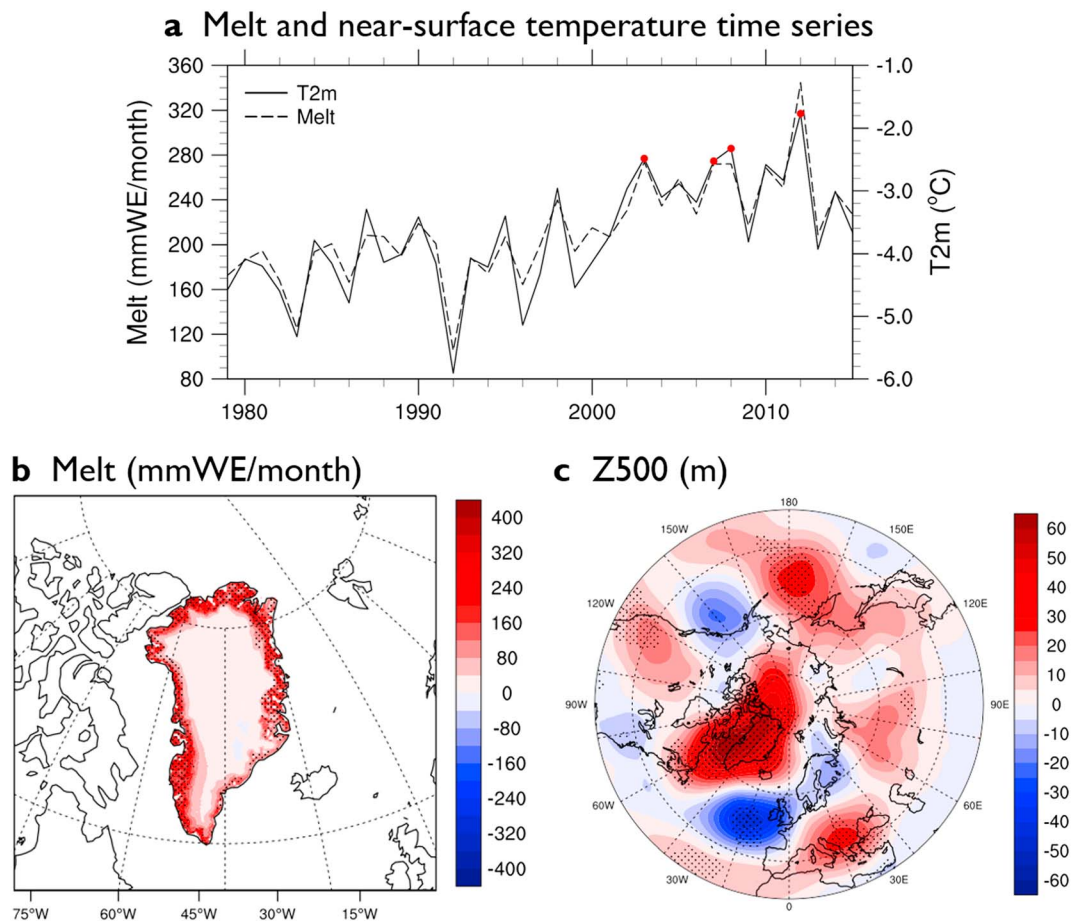
Figure 1. a) Time series of June–August (JJA) melt (mm water equivalent [mmWE]/month; dashed line) from the Modèle Atmosphérique Régional simulation and June–August near-surface temperature at 2-m height (T2m; °C; solid line) from ERA-Interim reanalysis averaged over Greenland for 1979–2015, with red dots indicating summers with extreme melt, defined as those with T2m in the top decile. JJA composite anomalies for top decile melt summers relative to the 1980–2009 mean for (b) melt (mmWE/month) and (c) Z500 (m). Stippling indicates anomalies statistically significant at the 95% confidence level.

surface melt particularly for the past few decades, we analyze the extent to which these links are present in the absence of anthropogenic forcing and whether global warming will change or supersede these links in the future.

2. Data and Methods

2.1. Model and Reanalysis Data

To investigate links between Greenland melt and natural variability under various greenhouse forcing scenarios, we primarily use the fully coupled Community Earth System Model version 1 Large Ensemble (CESM1-LE; Kay et al., 2015). All 40 ensemble members are forced by the same time-varying external forcing but begin with different initial conditions. Therefore, these ensemble members exhibit distinct internal variability and thus different phasing of the NAO and AMO. The ensemble is run with historical forcing from 1920 to 2005 (hereafter CESM1 HIST) and with RCP8.5 forcing from 2006 to 2100 (hereafter CESM1 RCP8.5) following the Coupled Model Intercomparison Project Phase 5 (CMIP5) protocol. We additionally use the 10-member CESM1 Global Ocean-Global Atmosphere experiment from 1920 to 2015 (hereafter CESM1 ATM), in which atmosphere and land model components are identical to the fully coupled CESM1, but ocean and sea ice components are inactive, instead using SST from the National Oceanic and Atmospheric Administration Extended Reconstructed Sea Surface Temperature and sea ice from the Hadley Centre Sea Ice and Sea Surface Temperature data set (HadISST). CESM1 ATM is run with historical forcing identical to CESM1 HIST from 1920 to 2005 and with RCP8.5 forcing from 2006 to 2015. Lastly, the fully coupled

CESM1 simulation with fixed 1850 preindustrial radiative forcing (hereafter CESM1 PI), which otherwise uses the same configuration as the CESM1-LE, allows for investigation of preindustrial conditions.

As shown by Vizcaíno et al. (2013), CESM1 realistically reproduces Greenland surface climate conditions in comparison to a regional climate model. In comparison with ERA-Interim and Modern-Era Retrospective analysis for Research and Applications, Version 2, the two reanalyses most consistent with observations of surface air temperatures over Greenland (Eyre & Zeng, 2017; Lindsay et al., 2014), CESM1 is significantly colder for the reference period 1980–2009 (Figures S1a and S1b in the supporting information). This cold bias may be related to CESM1's underestimation of Greenland blocking, although the model produces summer 500-hPa geopotential height (Z500) mean and variance patterns similar to the reanalyses (not shown) and shows Greenland blocking anomalies similar to those in ERA-Interim for high melt years from 1980 to 2009 (Figure 2). The temperature trends and number of extremes per decade for the 1980–2009 period in CESM1 are within range of the reanalysis products, further confirming the utility of CESM1 for this study. Both the fully coupled CESM1 HIST and atmosphere-only CESM1 ATM runs for the 1980–2009 period show median summer GrIS temperatures and 15-year temperature trends at or above the 75% quantile of their 1920–1949 counterparts and of the preindustrial experiment (CESM1 PI; Figures S1b and S1c). This warming signal is also evident in the evolution of the clustering of extreme temperature years, where there are more high melt summers and fewer low melt summers per decade for 1980–2009 compared to 1920–1949, a precursor to the 7 °C summertime warming over Greenland projected by CESM1 RCP8.5 by the end of the 21st century (Figures S1a, S1d, and S1e).

In comparison with the CESM1 simulations, reanalysis and observational data sets as well as a regional climate model simulation over Greenland are used. Surface melt in recent decades is provided by the Modèle Atmosphérique Régional version 3.5.2 regional climate model simulation for the GrIS (Fettweis et al., 2017). In addition, we use atmospheric temperature and geopotential height from the European Centre for Medium-Range Weather Forecasts Interim Reanalysis (ERA-Interim; Dee et al., 2011) and Modern-Era Retrospective analysis for Research and Applications, Version 2 (Molod et al., 2015) reanalysis data sets. We also use the HadISST data set (Rayner et al., 2003).

2.2. Climate Indices

The summer (June–August) GBI is calculated as the 500-hPa geopotential height area-averaged for 60°N to 80°N and 20°W to 80°W and time averaged for the summer season following Hanna et al. (2013). For the summer North Atlantic Oscillation (June–August NAO), the Hurrell (1995) station-based index definition is used, while the AMO is calculated by area averaging North Atlantic SST from 0°N to 60°N, removing the quadratic trend to exclude the climate change signal and computing the yearly average. We found similar AMO results using alternate methods of excluding the climate change signal, including linear detrending and removing the global mean SST (not shown).

3. Results

3.1. Atmospheric Variability and Greenland Melt

As established previously (Fettweis, Hanna, et al., 2013) and shown in Figure 1a, Greenland near-surface temperature and surface melt are highly correlated, motivating our use of near-surface temperature at 2-m height (T2m) as a proxy for melt. We investigate links between Greenland melt and atmospheric pressure conditions in different forcing scenarios by calculating geopotential height anomalies during summer melt seasons with Greenland T2m above the standard deviation for a given period in comparison to the full period (Figure 2).

Similar to the reanalysis for 1980–2009, the CESM1 fully coupled hindcast (HIST) and atmosphere-only hindcast (ATM) both exhibit anomalous high pressure over Greenland and low pressure to the southeast of Greenland characteristic of the negative NAO phase during extreme melt seasons. In fact, all CESM1 experiments and time periods show significant high-pressure anomalies over central Greenland during high melt summers, demonstrating an important role for natural variability in the form of the NAO regardless of external forcing. However, greenhouse gas forcing also appears to promote high melt as extreme melt years tend to occur near the end of the 1980–2009 and 2070–2099 periods, respectively. To isolate links between natural variability and Greenland melt, we remove the ensemble mean T2m and Z500 before choosing
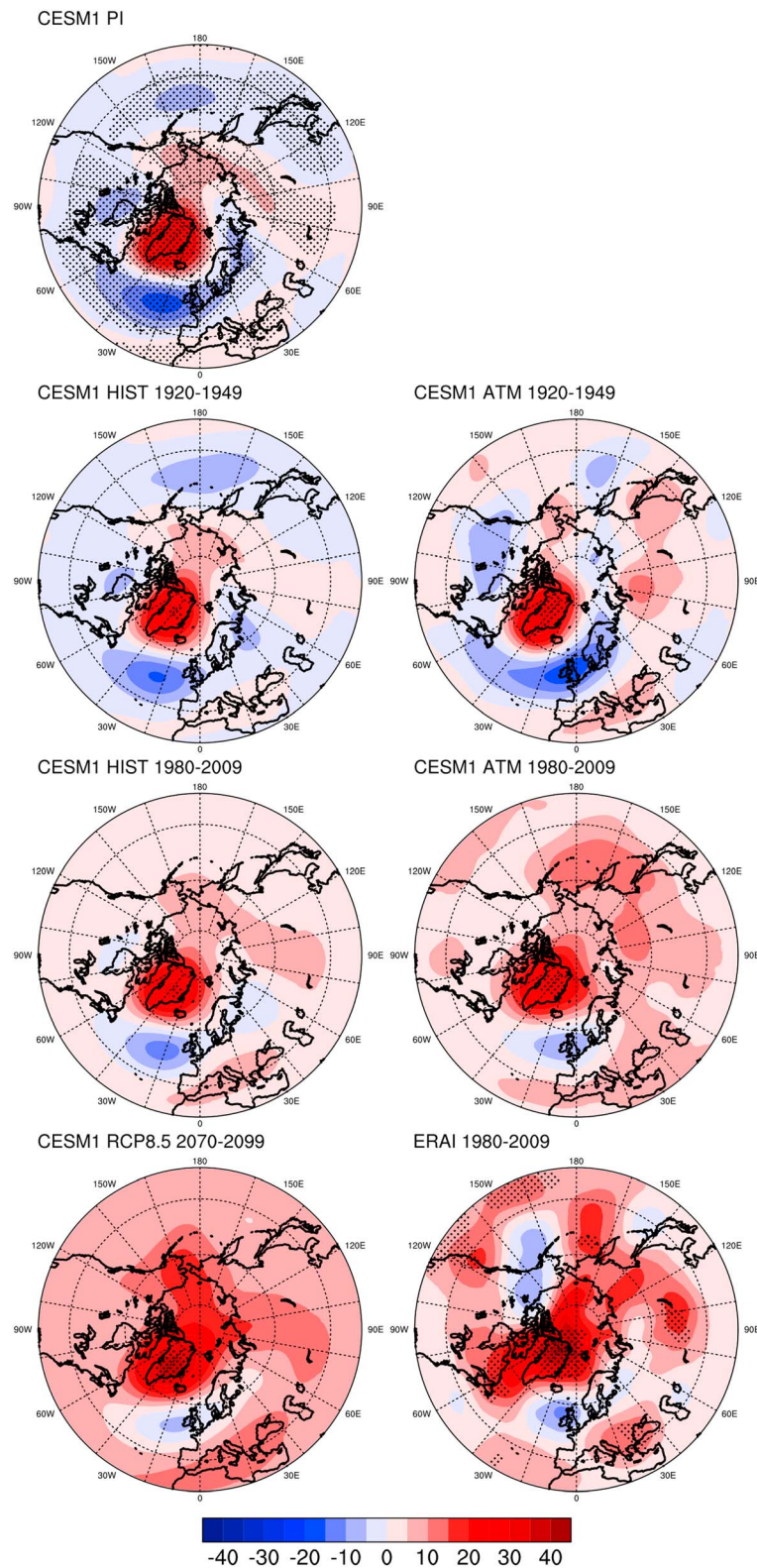
Figure 2. June–August Z500 anomalies (m) for extreme melt years with June–August GrIS T2m more than one standard deviation above the mean T2m for each period. Anomalies for CESM1 HIST, ATM, and RCP8.5 are calculated for each ensemble member before calculating the ensemble mean of anomalies. Stippling for CESM1 PI and ERA-Interim indicates anomalies statistically significant at the 95% confidence level; stippling for CESM1 HIST, ATM, and RCP8.5 indicates significance in at least 75% of composited ensemble members.
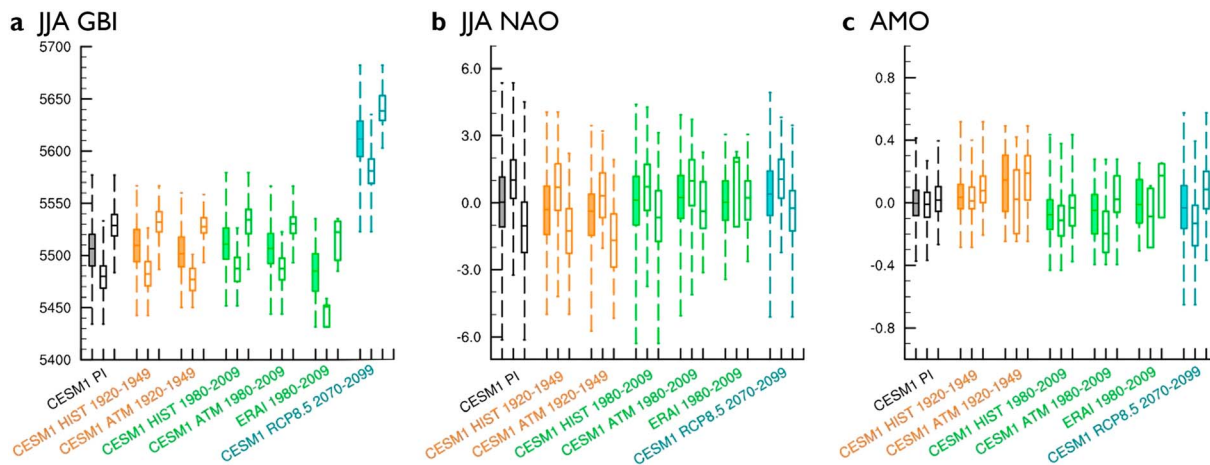
Figure 3. Climate indices for average conditions and for extreme GrIS summer melt years in CESM experiments and reanalysis. (a) June–August (JJA) Greenland Blocking Index (GBI), (b) JJA North Atlantic Oscillation index (NAO), and (c) Atlantic Multidecadal Oscillation index (AMO) for all years (left, filled box for each period), extremely low (middle box for each period), and extremely high (right box for each period) JJA Greenland T2m years, where JJA T2m for extreme years is more than one standard deviation above or below the mean T2m for a given period.

extreme melt years and calculating anomalies and find an even stronger NAO signal across the fully coupled large ensemble experiments, particularly for RCP8.5 2070–2099 (Figure S2).

This summertime NAO-melt connection in the CESM1 simulations is more symmetrically illustrated in Figure 3b, with high (low) melt years exhibiting a more negative (positive) NAO phase for all periods. We also plot the GBI (Figure 3a), a measure of high-pressure conditions over Greenland, as observations show a stronger correlation with Greenland melt for the GBI than the NAO (Hanna et al., 2013). High melt summers experience more frequent blocking conditions than low melt summers, with 75% of summers displaying no overlap in blocking values between the all, low, and high melt categories for all forcing scenarios. Behaving similarly to ERA-Interim, the much larger sets of data points for CESM1 experiments (Table S1) lend more statistical robustness to this result.

3.2. Oceanic Variability and Greenland Melt

In addition to the NAO, we investigate links between the AMO and melt under various greenhouse forcings by calculating SST anomalies during extreme melt seasons compared to each full period (Figures S3 and S4) and the AMO index for all, low, and high melt years (Figure 3c). While high melt seasons co-occur with warmer North Atlantic SSTs, the tripole structure of these anomalies for the fully coupled simulations (Figures S3 and S4) suggests that North Atlantic warming in high melt years is driven by the negative NAO rather than the AMO (Hurrell & Deser, 2010). Downward (upward) turbulent heat flux anomalies over warmer (colder) ocean regions during high melt seasons further suggest that NAO-related wind and heat fluxes predominantly force ocean temperatures (Figure S5).

However, the ocean influence on Greenland melt appears stronger in the reanalysis, as the warm SST anomalies in the subpolar gyre are damped by anomalous upward (negative) turbulent heat fluxes in ERAI (Figures S3 and S5). Similar heat flux patterns hold for CESM1 ATM for 1980–2009, which uses the observed SST anomalies as the boundary condition. Consistently, AMO index values are more distinct between low and high melt years for the observed SST (i.e., CESM1 ATM and HadISST) than for the fully coupled CESM1 PI and HIST (Figure 3c). Therefore, the fully coupled models may be underestimating the observed AMO impact on Greenland melt.

3.3. Impact of Natural Variability on Emergence of Widespread Greenland Melt

Our results so far establish a strong link between interannual Greenland melt variability, the summer NAO phase, and North Atlantic SSTs for all periods. We now investigate how the timing of NAO and AMO phases in different ensemble members, overlaid onto identical external forcing, may impact the emergence of widespread Greenland melt in a warming climate. Early and late emergence ensemble members are identified

AGU
100
ADVANCING EARTH
AND SPACE SCIENCE

Geophysical Research Letters

10.1029/2018GL079682
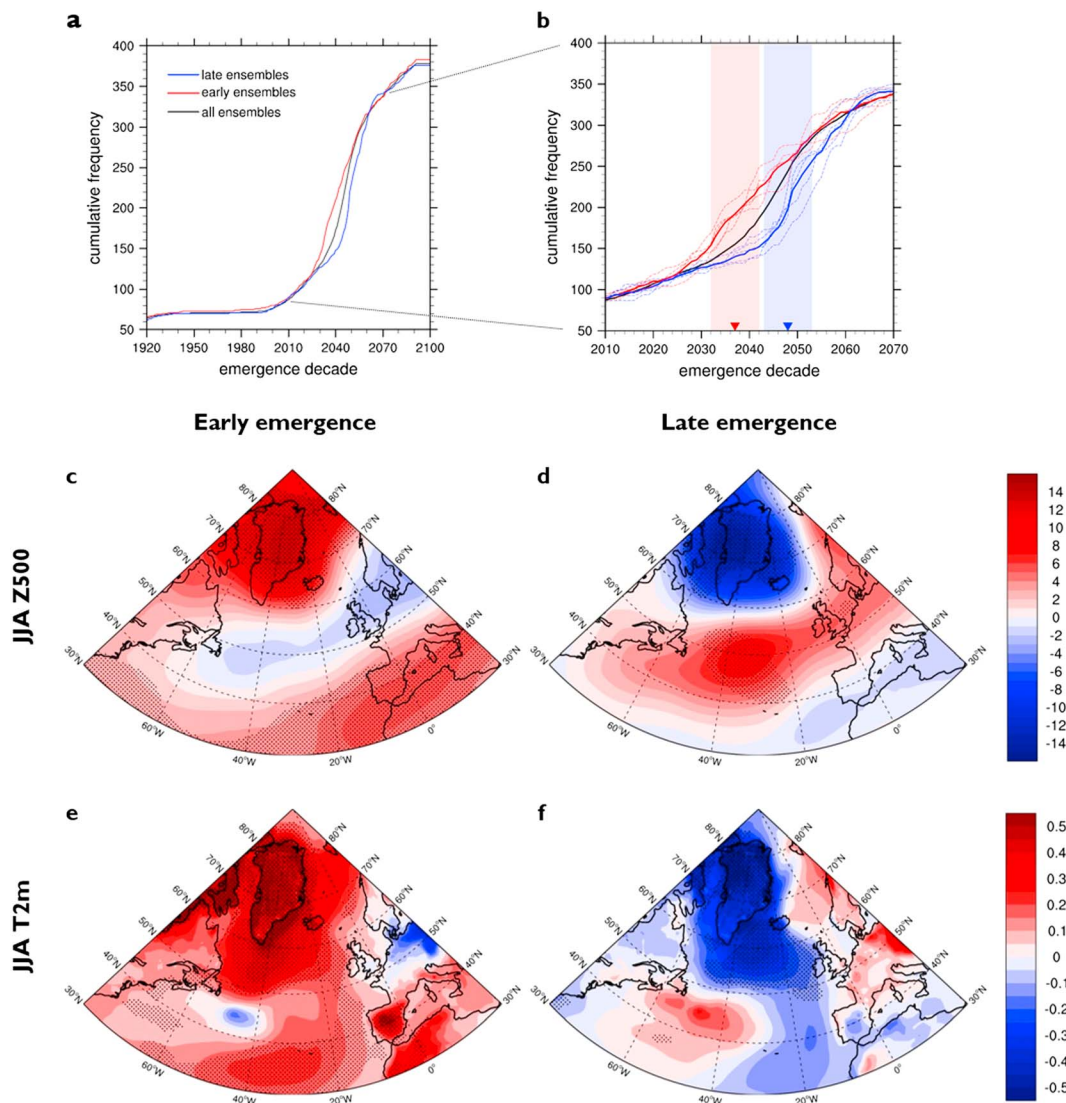
Figure 4. Timing of widespread Greenland Ice Sheet melt under global warming and associated circulation and temperature anomalies over the North Atlantic sector. (a) Number of grid points over the Greenland Ice Sheet with at least 7 years per decade above 0 °C, accumulated in time beginning in 1920 for each CESM1 HIST and RCP8.5 ensemble member and averaged for early emergence (red), late emergence (blue), and all (black) ensemble members. (b) As in (a), with individual early and late emergence ensemble members (dashed), triangle for the average emergence year for early (red) and late (blue) emergence members, and shading for 10-year emergence periods surrounding this year. Anomalies for each extreme emergence ensemble member compared to the ensemble average during emergence periods are averaged for early members and for late members to produce (c), (d) June–August (JJA) Z500 (m), and (e, f) JJA T2m (°C) average anomalies. Stippling for (c)–(f) indicates anomalies statistically significant at the 95% confidence level.

based on a decadal-scale sum of potential melt grid points over Greenland for 1920–2100 in CESM1 HIST and RCP8.5. We calculate the number of grid points over Greenland with at least 7 years per decade with T2m above 0 °C, then accumulate this quantity in time beginning in 1920 for each CESM1 HIST and RCP8.5 ensemble member. Early and late emergence ensemble members fall outside a standard deviation threshold on the distribution of the timing when each ensemble member reaches a criterion for widespread melting, that is, 50% of its 2100 cumulative frequency value. We trialed thresholds of 1, 7, and 10 years per decade above 0 °C in addition to 25%, 50%, and 75% of the 2100 cumulative frequency value but found that the 50% and 75% thresholds produce better separation of cumulative frequency time series for early and late members than the 25% threshold (not shown). Variations using 1, 7, and 10 years per decade combined with 50% and 75% of the 2100 cumulative frequency value all produce similar patterns for geopotential height and near-surface temperature anomalies for early and late emergence ensembles (not shown).

Geopotential height and near-surface temperature anomalies are calculated for early (late) emergence members compared to the ensemble mean of all members for the same period. With all ensembles experiencing the same external forcing, early emergence members exhibit widespread melting conditions (when 50% of the cumulative melt area from 1920 to 2100 is reached) up to 16 years sooner than late emergence members (Figures 4a–4b). In the decade surrounding the average emergence year, early (late) members show a more negative (positive) NAO phase and warmer (colder) North Atlantic temperatures than the ensemble mean for the same period (Figures 4c–4f), suggesting an important role for natural variability in impacting the timing of widespread Greenland melt.

4. Conclusions

We find strong links between summer Greenland melt and the NAO and AMO under all greenhouse forcing scenarios. Although ocean temperatures generally appear to be driven by the NAO signal during high melt summers, experiments with observational SSTs show a potentially stronger ocean influence on Greenland melt than the fully coupled experiments. Lastly, we find that under identical external forcing, ensemble members' disparate timing of emergence of widespread melt depends on the timing of modes of natural variability.

As natural variability appears important for Greenland melt in the past, present, and future, more accurate prediction of future Greenland melt hinges on understanding how modes of natural variability like the NAO and AMO may respond to greenhouse gas forcing. While the sign of the summer NAO does not look significantly different for 2070–2099 in comparison to past periods in CESM1-LE (Figure 3b), the CMIP5 ensemble mean projects a slightly more positive summer NAO under future greenhouse gas forcing (Fettweis, Hanna, et al., 2013). However, the CMIP5 models are known to generally underestimate observed blocking in the high-latitude North Atlantic and Europe (Anstey et al., 2013; Dunn-Sigouin & Son, 2013; Masato et al., 2013; Hanna, Fettweis, & Hall, 2018), calling into question their ability to project future NAO changes and highlighting a need for better model representation of blocking and further study into the impacts of climate change on natural variability. An additional open question concerns the relative importance of different mechanisms for connecting high-pressure conditions to extreme Greenland melt in different periods, as even for recent decades the mechanisms of warm air advection, cloud and radiative impacts, and large-scale sinking and adiabatic warming have all been implicated (Ding et al., 2017; Fettweis et al., 2011; Hofer et al., 2017; Lim et al., 2016). Furthermore, determining the extent to which the AMO impacts Greenland blocking and melt will be particularly important as the AMO phase and strength evolve in the future. Further study of natural variability links to Greenland melt is essential for predicting the climate response to greenhouse gas forcing.

References

Anstey, J. A., Davini, P., Gray, L. J., Woollings, T. J., Butchart, N., Cagnazzo, C., et al. (2013). Multi-model analysis of Northern Hemisphere winter blocking: Model biases and the role of resolution. *Journal of Geophysical Research: Atmospheres*, *118*, 3956–3971. https://doi.org/10.1002/jgrd.50231

Böning, C. W., Behrens, E., Biastoch, A., Getzla, K., & Bamber, J. L. (2016). Emerging impact of Greenland meltwater on deepwater formation in the North Atlantic Ocean. *Nature Geoscience*, *9*(7), 523–527. https://doi.org/10.1038/ngeo2740

Box, J. E., Fettweis, X., Stroeve, J. C., Tedesco, M., Hall, D. K., & Steffen, K. (2012). Greenland ice sheet albedo feedback: Thermodynamics and atmospheric drivers. *The Cryosphere*, *6*(4), 821–839. https://doi.org/10.5194/tc-6-821-2012

Chylek, P., Box, J. E., & Lesins, G. (2004). Global warming and the Greenland ice sheet. *Climatic Change*, *63*(1/2), 201–221. https://doi.org/10.1023/B:CLIM.0000018509.74228.03

Chylek, P., Folland, C. K., Lesins, G., Dubey, M. K., & Wang, M. (2009). Arctic air temperature change amplification and the Atlantic Multidecadal Oscillation. *Geophysical Research Letters*, *36*, L14801. https://doi.org/10.1029/2009GL038777

Dee, D. P., Uppala, S. M., Simmons, A. J., Berrisford, P., Poli, P., Kobayashi, S., et al. (2011). The ERA Interim reanalysis: Configuration and performance of the data assimilation system. *Quarterly Journal of the Royal Meteorological Society*, *137*(656), 553–597. https://doi.org/10.1002/qj.828

Ding, Q., Schweiger, A., L'Heureux, M., Battisti, D. S., Po-Chedley, S., Johnson, N. C., et al. (2017). Influence of high-latitude atmospheric circulation changes on summertime Arctic sea ice. *Nature Climate Change*, *7*(4), 289–295. https://doi.org/10.1038/nclimate3241

Ding, Q., Wallace, J. M., Battisti, D. S., Steig, E. J., Gallant, A. J. E., Kim, H.-J., & Geng, L. (2014). Tropical forcing of the recent rapid Arctic warming in northeastern Canada and Greenland. *Nature*, *509*(7499), 209–212. https://doi.org/10.1038/nature13260

Dunn-Sigouin, E., & Son, S.-W. (2013). Northern Hemisphere blocking frequency and duration in the CMIP5 models. *Journal of Geophysical Research: Atmospheres*, *118*, 1179–1188. https://doi.org/10.1002/jgrd.50143

Eyre, J. R., & Zeng, X. (2017). Evaluation of Greenland near surface air temperature datasets. *The Cryosphere*, *11*(4), 1591–1605. https://doi.org/10.5194/tc-11-1591-2017

Fettweis, X., Box, J. E., Agosta, C., Amory, C., Kittel, C., Lang, C., et al. (2017). Reconstructions of the 1900–2015 Greenland ice sheet surface mass balance using the regional climate MAR model. *The Cryosphere*, *11*(2), 1015–1033. https://doi.org/10.5194/tc-11-1015-2017

Fettweis, X., Franco, B., Tedesco, M., van Angelen, J. H., Lenaerts, J. T. M., van den Broeke, M. R., & Gallée, H. (2013). Estimating the Greenland ice sheet surface mass balance contribution to future sea level rise using the regional atmospheric climate model MAR. *The Cryosphere*, *7*(2), 469–489. https://doi.org/10.5194/tc-7-469-2013

Fettweis, X., Hanna, E., Lang, C., Belleflamme, A., Erpicum, M., & Gallée, H. (2013). Brief communication "Important role of the mid-tropospheric atmospheric circulation in the recent surface melt increase over the Greenland ice sheet". *The Cryosphere*, *7*(1), 241–248. https://doi.org/10.5194/tc-7-241-2013

Fettweis, X., Mabille, G., Erpicum, M., Nicolay, S., & Van den Broeke, M. (2011). The 1958–2009 Greenland ice sheet surface melt and the mid-tropospheric atmospheric circulation. *Climate Dynamics*, *36*(1-2), 139–159. https://doi.org/10.1007/s00382-010-0772-8

Gastineau, G., & Frankignoul, C. (2015). Influence of the North Atlantic SST variability on the atmospheric circulation during the twentieth century. *Journal of Climate*, *28*(4), 1396–1416. https://doi.org/10.1175/JCLI-D-14-00424.1

Häkkinen, S., Hall, D. K., Shuman, D. A., Worthen, D. L., & DiGirolamo, N. E. (2014). Greenland ice sheet melt from MODIS and associated atmospheric variability. *Geophysical Research Letters*, *41*, 1600–1607. https://doi.org/10.1002/2013GL059185

Häkkinen, S., Rhines, P. B., & Worthen, D. L. (2011). Atmospheric blocking and Atlantic Multidecadal Ocean variability. *Science*, *334*(6056), 655–659. https://doi.org/10.1126/science.1205683

Hanna, E., Cropper, T. E., Hall, R. J., & Cappelen, J. (2016). Greenland blocking index 1851–2015: A regional climate change signal. *International Journal of Climatology*, *36*(15), 4847–4861. https://doi.org/10.1002/joc.4673

Hanna, E., Fettweis, X., & Hall, R. J. (2018). Recent changes in summer Greenland blocking captured by none of the CMIP5 models. *The Cryosphere Discuss*, 1–8. https://doi.org/10.5194/tc-2018-91

Hanna, E., Fettweis, X., Mernild, S. H., Cappelen, J., Ribergaard, M. H., Shuman, C. A., et al. (2014). Atmospheric and oceanic climate forcing of the exceptional Greenland ice sheet surface melt in summer 2012. *International Journal of Climatology*, *34*(4), 1022–1037. https://doi.org/10.1002/joc.3743

Hanna, E., Hall, R. J., Cropper, T. E., Ballinger, T. J., Wake, L., Mote, T., & Cappelen, J. (2018). Greenland Blocking Index daily series 1851–2015: Analysis of changes in extremes and links with North Atlantic and UK climate variability and change. *International Journal of Climatology*, *38*(9), 3546–3564. https://doi.org/10.1002/joc.5516

Hanna, E., Jones, J. M., Cappelen, J., Mernild, S. H., Wood, L., Steffen, K., & Huybrechts, P. (2013). The influence of North Atlantic atmospheric and oceanic forcing effects on 1900–2010 Greenland summer climate and ice melt/runoff. *International Journal of Climatology*, *33*(4), 862–880. https://doi.org/10.1002/joc.3475

Hofer, S., Tedstone, A. J., Fettweis, X., & Bamber, J. L. (2017). Decreasing cloud cover drives the recent mass loss on the Greenland ice sheet. *Science Advances*, *3*(6), 1700584. https://doi.org/10.1126/sciadv.1700584

Hurrell, J. W. (1995). Decadal trends in the North Atlantic oscillation: Regional temperatures and precipitation. *Science*, *269*(5224), 676–679. https://doi.org/10.1126/science.269.5224.676

Hurrell, J. W., & Deser, C. (2010). North Atlantic climate variability: The role of the North Atlantic Oscillation. *Journal of Marine Systems*, *78*(1), 28–41. https://doi.org/10.1016/j.jmarsys.2008.11.026

Kay, J. E., Deser, C., Phillips, A., Mai, A., Hannay, C., Strand, G., et al. (2015). The Community Earth System Model (CESM) large ensemble project: A community resource for studying climate change in the presence of internal climate variability. *Bulletin of the American Meteorological Society*, *96*(8), 1333–1349. https://doi.org/10.1175/BAMS-D-13-00255.1

Lim, Y.-K., Schubert, S. D., Nowicki, S. M. J., Lee, J. N., Molod, A. M., Cullather, R. I., et al. (2016). Atmospheric summer teleconnections and Greenland ice sheet surface mass variations: Insights from MERRA-2. *Environmental Research Letters*, *11*(2), 024002. https://doi.org/10.1088/1748-9326/11/2/024002

Lindsay, R., Wensnahan, M., Schweiger, A., & Zhang, J. (2014). Evaluation of seven different atmospheric reanalysis products in the Arctic. *Journal of Climate*, *27*(7), 2588–2606. https://doi.org/10.1175/JCLI-D-13-00014.1

Masato, G., Hoskins, B. J., & Woollings, T. (2013). Winter and summer Northern Hemisphere blocking in CMIP5 models. *Journal of Climate*, *26*(18), 7044–7059. https://doi.org/10.1175/JCLI-D-12-00466.1

McLeod, J. T., & Mote, T. L. (2016). Linking interannual variability in extreme Greenland blocking episodes to the recent increase in summer melting across the Greenland ice sheet. *International Journal of Climatology*, *36*, 1484–1499. https://doi.org/10.1002/joc.4440

Molod, A., Takacs, L., Suarez, M., & Bacmeister, J. (2015). Development of the GEOS-5 atmospheric general circulation model: Evolution from MERRA to MERRA2. *Geoscientific Model Development*, *8*(5), 1339–1356. https://doi.org/10.5194/gmd-8-1339-2015

Oltmanns, M., Karstensen, J., & Fischer, J. (2018). Increased risk of a shutdown of ocean convection posed by warm North Atlantic summers. *Nature Climate Change*, *8*(4), 300–304. https://doi.org/10.1038/s41558-018-0105-1

Peings, Y., & Magnusdottir, G. (2014). Forcing of the wintertime atmospheric circulation by the multidecadal fluctuations of the North Atlantic Ocean. *Environmental Research Letters*, *9*(3), 034018. https://doi.org/10.1088/1748-9326/9/3/034018

Rahmstorf, S., Box, J. E., Feulner, G., Mann, M. E., Robinson, A., Rutherford, S., & Schaffernicht, E. J. (2015). Exceptional twentieth-century slowdown in Atlantic Ocean overturning circulation. *Nature Climate Change*, *5*(5), 475–480. https://doi.org/10.1038/NCLIMATE2554

Rayner, N. A., Parker, D. E., Horton, E. B., Folland, C. K., Alexander, L. V., Rowell, D. P., et al. (2003). Global analyses of sea surface temperature, sea ice, and night marine air temperature since the late nineteenth century. *Journal of Geophysical Research*, *108*(D14), 4407. https://doi.org/10.1029/2002JD002670

Shepherd, A., Ivins, E. R., A, G., Barletta, V. R., Bentley, M. J., Bettadpur, S., et al. (2012). A reconciled estimate of ice-sheet mass balance. *Science*, *338*(6111), 1183–1189. https://doi.org/10.1126/science.1228102

Straneo, F., & Heimbach, P. (2013). North Atlantic warming and the retreat of Greenland's outlet glaciers. *Nature*, *504*(7478), 36–43. https://doi.org/10.1038/nature12854

Tedesco, M., Mote, T., Fettweis, X., Hanna, E., Jeyaratnam, J., Booth, J. F., et al. (2016). Arctic cut-off high drives the poleward shift of a new Greenland melting record. *Nature Communications*, *7*, 11723. https://doi.org/10.1038/ncomms11723

Vizcaíno, M., Lipscomb, W. H., Sacks, W. J., van Angelen, J. H., Wouters, B., & van den Broeke, M. R. (2013). Greenland surface mass balance as simulated by the Community Earth System model. Part I: Model evaluation and 1850–2005 results. *Journal of Climate*, *26*(20), 7793–7812. https://doi.org/10.1175/JCLI-D-12-00615.1